ACADEMIC PRESS

Available online at www.sciencedirect.com

SCIENCE DIRECT®

Journal of Sound and Vibration 262 (2003) 1153–1170

JOURNAL OF SOUND AND VIBRATION

www.elsevier.com/locate/jsvi

Vibration analysis of annular-like plates

L. Cheng*, Y.Y. Li, L.H. Yam

Department of Mechanical Engineering, The Hong Kong Polytechnic University, Hung Hom, Kowloon, Hong Kong

Received 10 January 2002; accepted 1 July 2002

Abstract

The existence of eccentricity of the central hole for an annular plate results in a significant change in the natural frequencies and mode shapes of the structure. In this paper, the vibration analysis of annular-like plates is presented based on numerical and experimental approaches. Using the finite element analysis code *Nastran*, the effects of the eccentricity, hole size and boundary condition on vibration modes are investigated systematically through both global and local analyses. The results show that analyses for perfect symmetric conditions can still roughly predict the mode shapes of "recessive" modes of the plate with a slightly eccentric hole. They will, however, lead to erroneous results for "dominant" modes. In addition, the residual displacement mode shape is verified as an effective parameter for identifying damage occurring in plate-like structures. Experimental modal analysis on a clamped–free annular-like plate is performed, and the results obtained reveal good agreement with those obtained by numerical analysis. This study provides guidance on modal analysis, vibration measurement and damage detection of plate-like structures.

1. Introduction

Circular plates with cutouts are extensively used in mechanical structures. Vibration analysis of this kind of structure is the foundation for structural parameter identification, damage detection and vibration control. In general, most research work has focused on vibration analysis of circular plates with a central hole, i.e., annular plates, and has led to a rapid development of analytical or experimental methods, such as the energy approach, the mode subtraction approach, etc. [1–8].

However, for engineering applications, many machine elements or structural components can be modelled as a circular plate with eccentric holes, i.e., the annular-like plate. Usually, due to the influence of asymmetry, the vibration behaviour of these structures will deviate significantly from that of the annular plate, e.g., the split of doublet frequencies and the distortion of mode shapes.

*Corresponding author. Fax: +852-2365-4703.
E-mail address: mmlcheng@polyu.edu.hk (L. Cheng).

0022-460X/03/$ - see front matter
doi:10.1016/S0022-460X(02)01093-3

In such cases, vibration analysis of annular-like plates has been a topic of practical interest and attracted much attention [9–11]. For example, by using the finite element method, Khurasia and Rawtant [10] examined the effect of variation in eccentricity on vibration behaviour for an annular-like plate. Chen and Zhou [11] illustrated the low-frequency mode shapes of a small disc with eccentric holes based on the boundary element approach.

As is known, the existence of eccentric holes in circular plates will lead to the splitting of doublet frequencies obtained for annular plates, and consequently affect the vibration modes of the structure. In such cases, the influence of eccentricity on repeated frequencies or mode shapes should be considered carefully during modal analysis. From the analyses of Khurasia et al. [10] and Chen et al. [11], it can be seen that the presented results are deficient because they disregard the influence of repeated frequencies and mode shapes. Some indications in this connection can be found from the work of Tseng and Wickert [12] using an eccentrically clamped annular plate, which showed that each pair of repeated frequencies splits at a rate that depends on the number of nodal diameters with increasing eccentricity.

However, as for the effects of variation of eccentricity, hole size and boundary condition on vibration modes during modal analysis, scanty literature is available and very few results have yet been reported on numerical or experimental analysis. In addition, from the results of Wong et al. [8], which show that a significant change at the circumference of the hole can be perceived from the residual displacement mode shape (DMS), defined as the difference of DMS between the circular and annular plates, it is of interest to know whether this conclusion is still valid for circular plates with an eccentric hole. This question is of particular relevance to the problem of damage detection.

The aim of this paper is to investigate these problems systematically. It attempts to reveal the relationship between parameter variations (eccentricity, hole size, boundary condition) and vibration modes, and to discover the vibration behaviour around the eccentric hole. To our knowledge, these results are new and give guidance for the modal analysis and damage detection of circular plates. The paper is organized as follows. In Section 2, the theoretical foundation of vibration analysis around the hole of an annular-like plate is introduced. In Section 3, numerical studies on the effects of the eccentricity, the hole size and the boundary conditions on vibration modes is discussed systematically from both global and local points of view. In order to verify the validity of the numerical analysis, experimental modal analysis is carried out in Section 4 for a clamped–free steel plate with eccentricity. Techniques on the construction of an ideal boundary condition and the selection of an excitation location are described. Finally, some constructive conclusions are drawn.

2. Theoretical background

2.1. Mode shape of an annular-like plate

Consider the annular-like plate shown in Fig. 1: its *ij*th displacement mode shape $W_{ij}(r,\alpha)$ in the polor coordinate can be expressed as

$$W_{ij}(r,\alpha) = \psi_{ij}(r)\Theta_{ij}(\alpha), \tag{1}$$

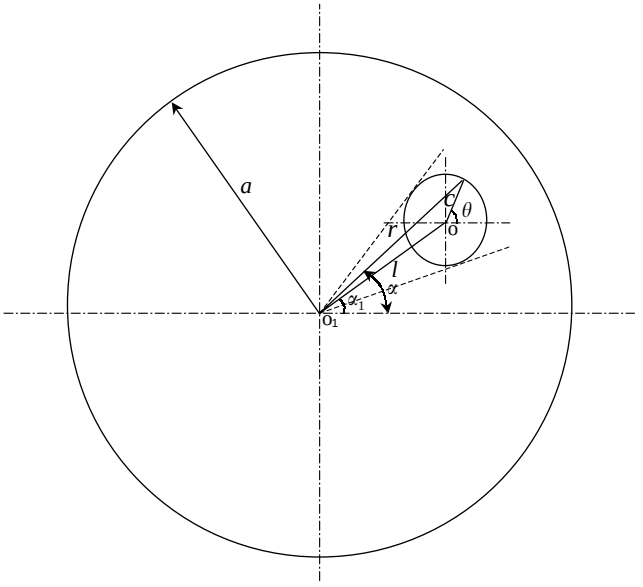

Fig. 1. Schematic diagram of the annular-like plate.

where i, j are the numbers of nodal diameters and circles, and $\psi_{ij}(r)$ and $\Theta_{ij}(\alpha)$ are the functions related to the polor radius r and polor angle α, respectively. For the annular case, $\psi_{ij}(r)$ can be expressed by the linear combination of Bessel functions. However, for the annular-like case, this expression is no longer valid. Thus, suitable shape functions should be used to describe $\psi_{ij}(r)$ and $\Theta_{ij}(\alpha)$. In general, some admissible shape functions, such as the pb-2 function and the bi-orthogonal basis can be utilized to form $\psi_{ij}(r)$ and $\Theta_{ij}(\alpha)$ [9].

2.2. Vibration behaviour at the circumference of the hole

The mode subtraction approach is manifested as an efficient tool in revealing vibration behaviour around the hole for annular plates [8]. In this section, the analysis will be extended to the vibration around the hole for annular-like plates.

As is known, the bending moment *at the free inner edge* satisfies

$$\begin{aligned} & M_{ij}(r,\alpha)\Big|_{\substack{r=r(l,c,\alpha)\\ \alpha_1-\arcsin(l/c)\leqslant\alpha\leqslant\alpha_1+\arcsin(l/c)}} \\ & = D\left(\frac{\partial^2 W_{ij}(r,\alpha)}{\partial r^2}+\nu\left[\frac{1}{r}\frac{\partial W_{ij}(r,\alpha)}{\partial r}+\frac{1}{r^2}\frac{\partial^2 W_{ij}(r,\alpha)}{\partial\alpha^2}\right]\right)\Bigg|_{\substack{r=r(l,c,\alpha)\\ \alpha_1-\arcsin(l/c)\leqslant\alpha\leqslant\alpha_1+\arcsin(l/c)}} \\ & = 0, \end{aligned} \tag{2}$$

where D, ν, c and l are flexible rigidity, the Poisson ratio, radius and eccentricity of the hole, respectively. The polor radius r is a function of the eccentricity l, the hole size c and the polor

angle α, and

$$r = r(l, c, \alpha) = l\cos(\theta - \alpha_1) + \sqrt{c^2 - l^2\sin^2(\alpha - \alpha_1)}. \tag{3}$$

In order to reveal the variation of DMSs around the hole using the mode subtraction approach, the ijth vibration mode of circular plates is denoted by [13]

$$W_{o,ij}(r, \alpha) = \psi_{o,ij}(r)\Theta_{o,ij}(\alpha) \quad (0 \leqslant r \leqslant a), \tag{4}$$

where $\psi_{o,ij}(r)$ is given by the linear combination of Bessel functions. For this case, the bending moment *at the virtual location* $r = r(l, c, \alpha)$ is not equal to zero, i.e.,

$$\begin{aligned} & M_{o,ij}(r, \alpha)\Big|_{\substack{r=r(l,c,\alpha) \\ \alpha_1 - \arcsin(l/c) \leqslant \alpha \leqslant \alpha_1 + \arcsin(l/c)}} \\ & = D\left(\frac{\partial^2 W_{o,ij}(r, \alpha)}{\partial r^2} + \nu\left[\frac{1}{r}\frac{\partial W_{o,ij}(r, \alpha)}{\partial r} + \frac{1}{r^2}\frac{\partial^2 W_{o,ij}(r, \alpha)}{\partial \alpha^2}\right]\right)\Bigg|_{\substack{r=r(l,c,\alpha) \\ \alpha_1 - \arcsin(l/c) \leqslant \alpha \leqslant \alpha_1 + \arcsin(l/c)}} \\ & = \varphi(l). \end{aligned} \tag{5}$$

Thus, with the help of Eqs. (2), (4) and (5), the difference between the circular and annular plates of the ijth DMS at the circumference of hole can be obtained as

$$\begin{aligned} & \Delta W_{ij}(r, \theta)\Big|_{\substack{r=r(l,c,\alpha) \\ \alpha_1 - \arcsin(l/c) \leqslant \alpha \leqslant \alpha_1 + \arcsin(l/c)}} \\ & = W_{o,ij}(r, \alpha) - W_{ij}(r, \alpha)\Big|_{\substack{r=r(l,c,\alpha) \\ \alpha_1 - \arcsin(l/c) \leqslant \alpha \leqslant \alpha_1 + \arcsin(l/c)}} \\ & = \nu\left\{\int\int\left[\frac{1}{r}\left(\psi'_{ij}(r)\Theta_{ij}(\alpha) - \psi'_{o,ij}(r)\Theta_{o,ij}(\alpha)\right)\right.\right. \\ & \left.\left. = +\frac{1}{r^2}\left(\psi_{ij}(r)\Theta''_{ij}(\alpha) - \psi_{o,ij}(r)\Theta''_{o,ij}(\alpha)\right)\right] \mathrm{d}r\mathrm{d}r\right\} + \tfrac{1}{2}\varphi(l)\cdot r^2\Big|_{\substack{r=r(l,c,\alpha) \\ \alpha_1 - \arcsin(l/c) \leqslant \alpha \leqslant \alpha_1 + \arcsin(l/c)}} \\ & i = 0, 1, \ldots, m;\ j = 0, 1, \ldots, n \end{aligned} \tag{6}$$

2.3. Discussion

1. Compared with the results obtained in Ref. [8] for the annular plate, the change in DMS around the hole is more complicated for the annular-like plate because of the variation of parameter r and the intricate expression of $\psi_{ij}(r)$ and $\Theta_{ij}(\alpha)$. Consequently, only the qualitative analysis of vibration around the hole can be described from Eq. (6).
2. When the eccentricity l/a approaches 0, i.e., the centre of hole ($\mathbf{o}$) is very close to the centre of the circular plate ($\mathbf{o_1}$), $\psi_{ij}(r)$ can degenerate into the form of a Bessel function. Under these circumstances, the results achieved for the annular case are valid for the annular-like case with a slight eccentricity. This can be verified from Fig. 2 with the consideration of the effect of l/a on natural frequencies and mode shapes. This is useful for practical applications; for example, the mismachining of an annular plate with a small deviation of the hole will not affect the vibration behaviour of the structure.

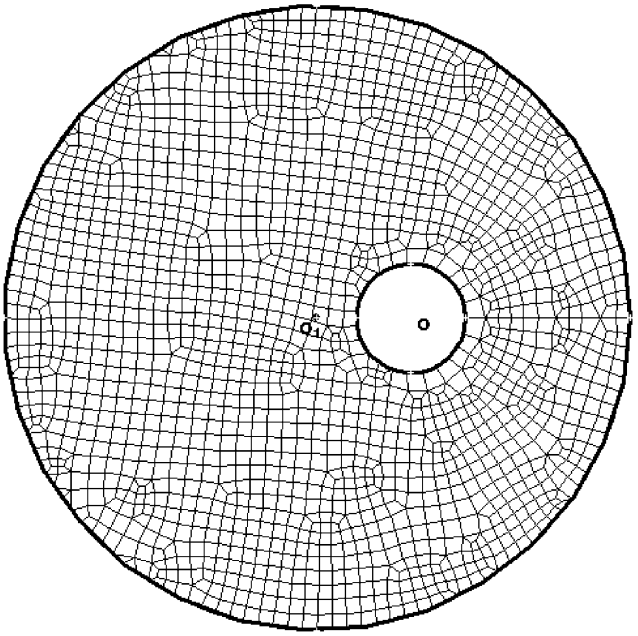

Fig. 2. Mesh elements of an annular-like plate constructed from the finite element analysis code *Nastran*.

3. Vibration analysis of an annular-like plate

As is known, vibration analysis of a symmetric structure, e.g., the circular or annular plate, results in the two-fold repeated frequencies occurring at mode (i,j) $(i = 1, 2, \ldots, m; j = 0, 1, \ldots, n)$, while for asymmetric structures such as the annular-like plate $(l/a \neq 0)$, the doublet frequency splits into two distinct values, which has a significant effect on mode shape. In this section, by using the numerical approach, the effects of the eccentricity, hole size and boundary condition on vibration modes with respect to the split and repeated frequencies are investigated in detail through global and local analyses.

Commercially available finite element code *Nastran* [14] was used to carry out the numerical simulations. Standard modelling procedure was followed to define the geometry, boundary conditions, material and element properties. For a given mesh size, quad elements and their corresponding nodes are generated automatically. In the present analysis, an annular-like plate with a diameter of 160 mm and a thickness of 0.7 mm was used. The eccentricity and hole size can take different values to simulate different cases of annular-like plates. For illustration purposes, the mesh grid of an annular-like plate ($l/a = 0.15$, $c/a = 0.15$) with a mesh size of 3.81 mm is shown in Fig. 2, in which 1649 plate elements and 1722 nodes are generated. As only lower order vibration modes are of interest in the present analysis, the mesh used is sufficiently refined to give accurate solutions.

3.1. Global analysis

A global analysis describes the vibration behaviour of the whole structure using the parameter of DMS. Before the analysis of the vibration mode, the effect of eccentricity l/a on frequencies is

first examined. Fig. 3(a) shows the *first several* natural frequencies of a clamped–free annular-like plate ($c/a = 0.25$) with l/a changing from 0, 0.15, 0.30, 0.45 to 0.6. A clamped condition is applied to the outer edge of the plate. It can be found that for modes with $i = 0$ (no nodal diameter), e.g., modes (0,0) and (0,1), single frequency is observed, which will be referred to as singlet frequency hereafter. For cases where $i \geq 1$, such as modes (1,0) and (2,0), the repeated frequency occurring in the annular plates ($l/a = 0$) is separated into two distinct values, which are referred to as the "dominant" and "recessive" frequencies, respectively. Obviously, the difference between these two values becomes significant with the increase of l/a.

3.1.1. *Effect of the eccentricity*

Fig. 3(b) shows the DMSs of a clamped circular plate ($c/a = 0$) and a clamped–free annular-like plate ($c/a = 0.25$) with eccentricity l/a changing from 0, 0.15, 0.30, 0.45 to 0.6. From this figure, some observations can be made as follows:

Symmetric cases when $c/a = 0$ (*the circular case*) *and* $l/a = 0$ (*the annular case*):

- In the case of singlet frequency ($i = 0$), only the nodal circle will be observed and the wave number is $2j$ for mode $(0,j)$ ($j = 1, \ldots, n$), with the exception of mode (0,0), for which no nodal circle is found.
- In the case of doublet frequency, the vibration mode occurs in pairs with the same shape, and the wave number is $2(i+j)$ ($i = 1, 2, \ldots, m; j = 0, 1, \ldots, n$). In addition, the nodal diameters retain straight even if they are broken at the hole section, and the nodal circles are unchanged.

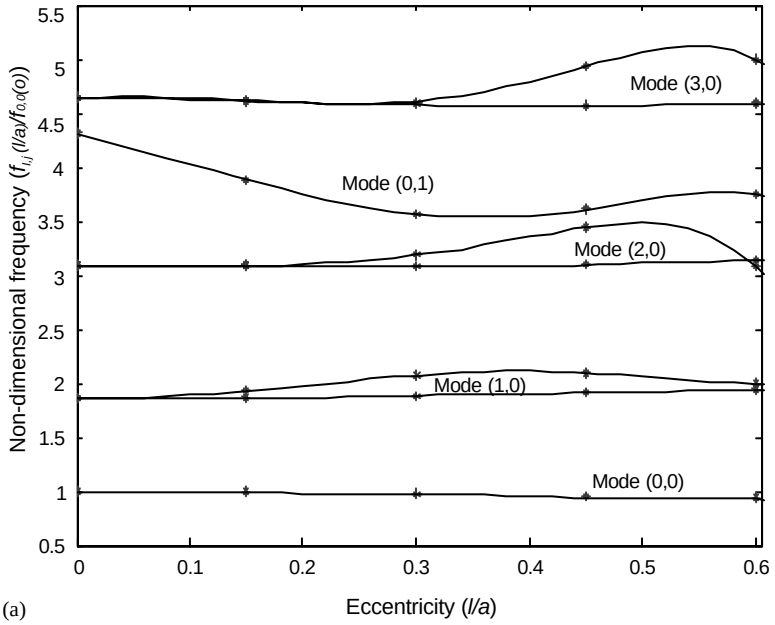

(a)

Fig. 3. (a) Effect of variation in l/a on natural frequencies, and (b) effect of variation in l/a on DMSs.

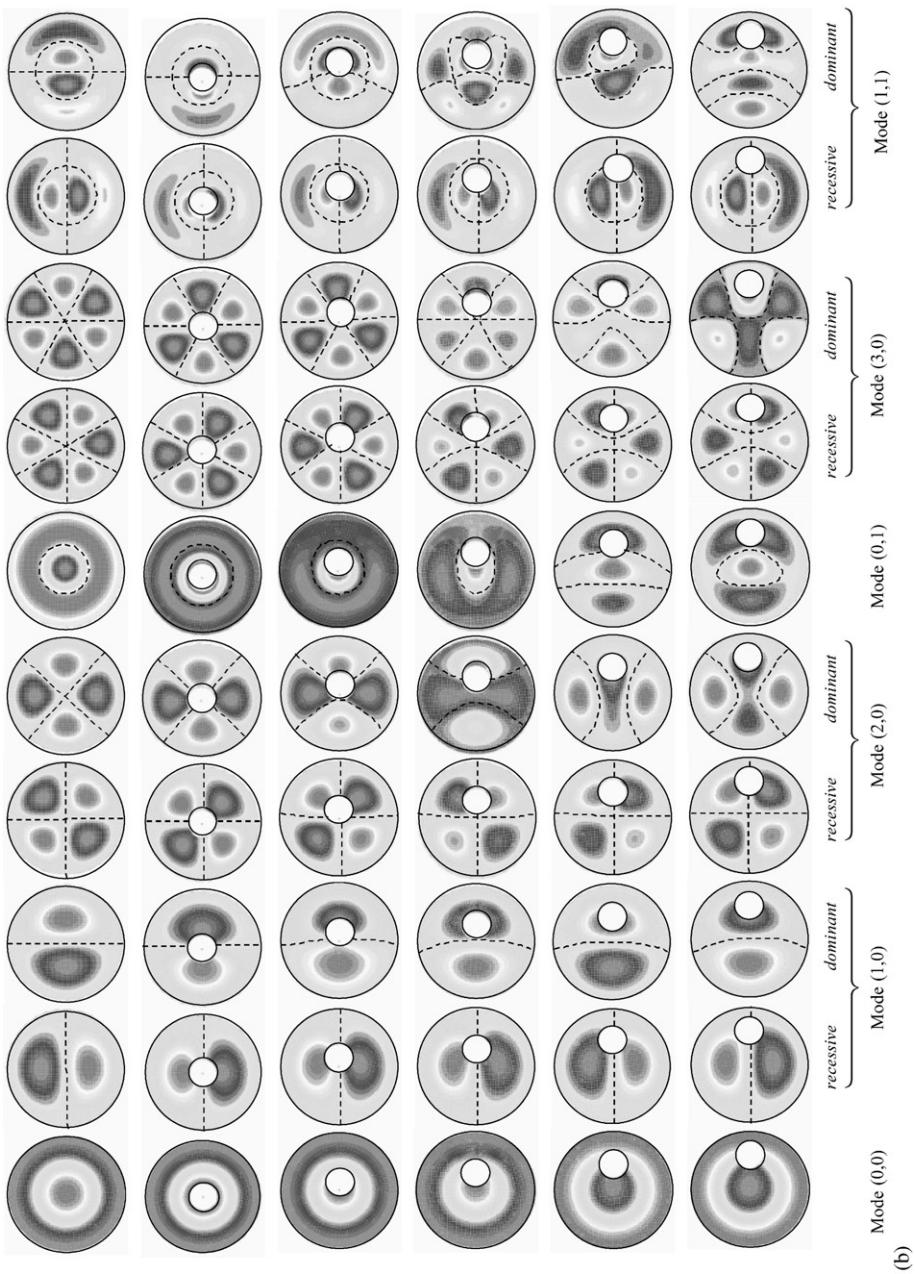

Fig. 3 (*continued*).

Asymmetric cases when $l/a \neq 0$ (the annular-like cases):

- In the case of singlet frequency (i=0), with the increase of eccentricity l/a, the nodal circles are flattened, then degenerated into nodal lines and recircled again (mode (0,1)). As a result, the mode shape changes remarkably compared with that of the annular case.
- In the case of "recessive" frequency, one of the nodal diameters will pass through the centre of the eccentric hole. The nodal diameters and circles remain unchanged or change slightly, and the mode shape retains its basic characteristic shape, i.e., no obvious variation of mode shapes is observed. For example, similar to the case of a circular or annular plate, the numbers of peaks are *two* for mode (1,0) and *four* for mode (2,0);
- In the case of "dominant" frequency, with the increase of l/a, the trends of nodal diameters and circles deviate from their origin, and their shapes are remarkably distorted, especially for high-order modes. For instance, the nodal diameter bends gradually for mode (1,0) and tends to be curvy for mode (2,0), while for modes (3,0) and (1,1), its shape changes completely. Obviously, a variation of mode shapes can be found when compared with their counterparts in circular or annular plates.

3.1.2. Effect of the hole size

The effect of hole size on mode shapes is discussed in this section. As mentioned above, for annular-like plates, due to "frequency splitting", the mode shape corresponding to the "recessive" one, defined as the "recessive" mode, retains its original shape, while that corresponding to the "dominant" one, defined as the "dominant" mode, changes obviously. This observation is also tenable for annular-like plates with a different size of hole. Therefore, only "dominant" modes will be taken for a concise analysis. Fig. 4 gives the mode shapes of a clamped–free annular-like plate ($l/a = 0.45$) with the hole size c/a changing from 0.1, 0.15, 0.2, 0.25 to 0.3. For modes $(i, 0)$ (i=1,2,3), the diameter lines bend gradually and degenerate into nodal lines. Special attention is paid to mode (2,0), in which two nodal lines for the case $c/a = 0.25$ rejoin as an opened nodal circle for the case of $c/a = 0.3$, whereas, for mode (0,1), the nodal circle is extended into two nodal lines. As for modes with coupled nodal diameters and circles, e.g., modes (1,1) and (2,1), this couple situation vanishes with the increase of c/a.

Obviously, with the increase of c/a, changes in the nodal diameters and circles are noticeable for the "dominant" case. As a result, the mode shapes differ remarkably from those obtained for the circular or annular plate. However, in the "recessive" case, global analysis reveals no obvious change for the same order of mode shape, no matter whether the structure is with or without an eccentric hole. In this case, the local analysis using mode subtraction approach will be performed to explore the vibration behaviour of the structure.

3.1.3. Effect of the boundary condition

In order to illustrate the influence of different boundary conditions on the aforementioned observations, the DMSs of a circular plate ($c/a = 0$) and an annular-like plate ($c/a = 0.25, l/a = 0.45$) under simply supported–free, free–free and partial clamped–free constraints are studied. Some results are plotted in Fig. 5 for comparison. Similar results to those presented in Section 3.1.1 for the clamped–free case can also be achieved for the simply supported-free and free–free cases. A common feature of these cases is that they are subjected to symmetric constraints.

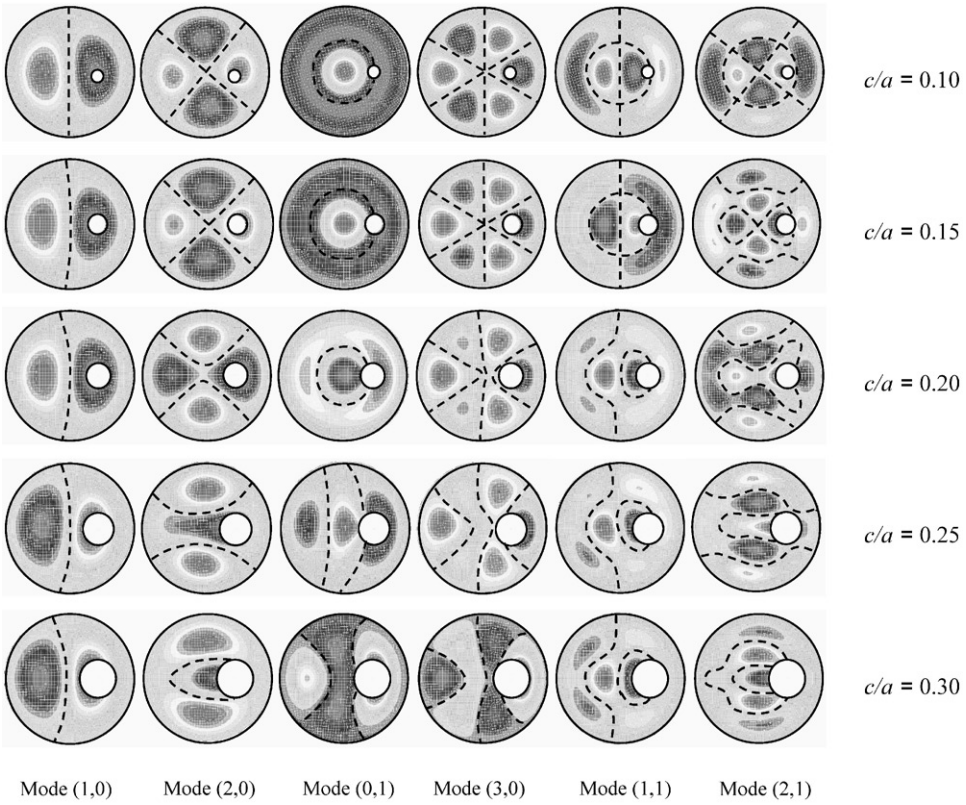

Fig. 4. Effect of variation in c/a on DMSs with eccentricity l/a=0.45.

For the asymmetric constraint, however, things have changed. This is demonstrated by the partial clamped–free case, in which a partial clamped–free constraint is realized by restricting the displacement and rotation at the clamped region of the outer boundary, while keeping them free at the inner boundary. In this example, three parts of the outer circumference at intervals [0, $\pi/12$], [$2\pi/3$, $3\pi/4$] and [$4\pi/3$, $7\pi/5$], as shown in Fig. 5(a), are fixed to simulate the clamped region. The results reveal that the repeated natural frequencies vanish regardless of whether or not the structure has an eccentric hole, and the wave number of $2(i+j)$ for mode (i,j) of the clamped case (Fig. 3(b), cases where $c/a = 0$ and $c/a = 0.25$, $l/a = 0.45$) is no longer satisfied for the same order mode of the partial–clamped case. Consequently, the asymmetric mode shapes are observed.

In summary, a noticeable difference in vibration modes can be found between structures with symmetric and asymmetric boundary conditions. For this reason, care should be taken in the configuration of an ideal boundary during the experimental analysis, so that accurate data can be acquired for modal analysis.

3.2. Local analysis

Local analysis aims to investigate the local vibration behaviour of the structure using the parameter of residual DMS. As presented in Ref. [8], the local technique was found to provide

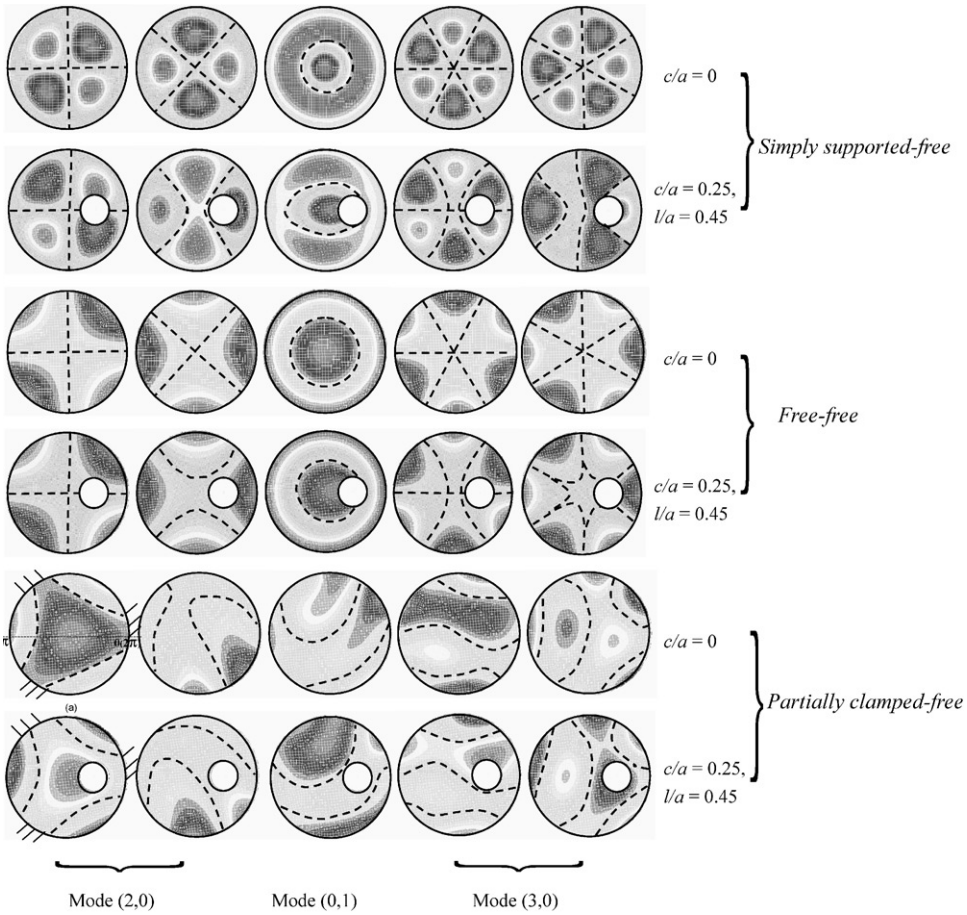

Fig. 5. Effect of different boundary conditions on DMSs.

efficient, accurate information on identifying the location of a hole (through the peak of the residual DMS) in the structure. This result is valuable for damage detection of plate-like structures. In this section, the local technique is extended to analyze the vibration behaviour of annular-like plates with consideration of the effects of the eccentricity and the hole size. Firstly, the DMSs of the circular and annular-like plates are identified and normalized by dividing the whole set of deflections by the maximum value. The residual DMS between these two cases can then be calculated, and the vibration behaviour at the circumference of the hole will be obtained. Due to the use of the subtraction technique, peaks appearing at those positions where the extreme amplitudes of modes are found inherently from global analysis will be eliminated from local analysis.

3.2.1. *Effect of the eccentricity*

Fig. 6 shows the contour of the residual DMSs at the circumference of the hole ($c/a = 0.25$) with the eccentricity l/a varying from 0, 0.15, 0.3, 0.45 to 0.6. For mode (1,0) (Fig. 5(a)), it can be

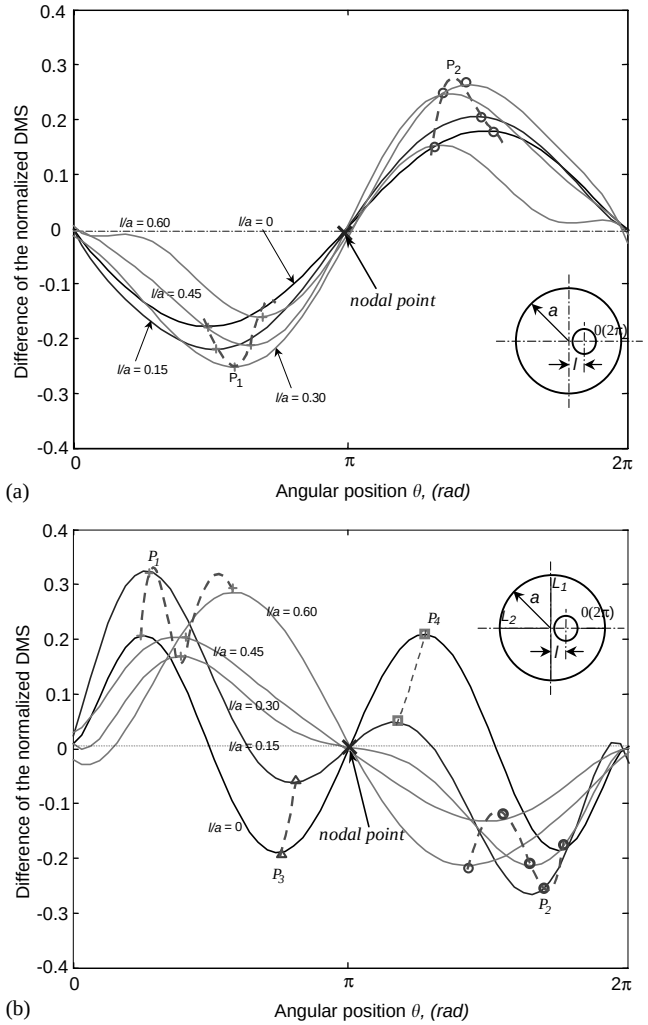

Fig. 6. Contour of DMSs around the hole with l/a varying from 0 to 0.6.

found that when the angular position θ varies from 0 to 2π, two peaks (p_1 and p_2) are observed, and with the increase of l/a, the amplitude of peaks increases first and then decreases with their positions moving toward the nodal point at location $\theta = \pi$ (the trace is shown by the dash lines). For mode (2,0) (Fig. 5(b)), four peaks ($p_1 - p_4$) are detected for the annular case ($l/a = 0$). However, with the increase of l/a from 0.15 to 0.6, peaks p_3 and p_4 disappear, and only p_1 and p_2 exist. The reason for this is that the effect of nodal line L_1 on vibration around the hole is weak when the eccentric hole is far away from L_1.

These results show that some peaks can be detected at the circumference of the hole from local analysis, and their number and locations depend on the eccentricity to a large extent. In addition, although there is no regular relationship between the variation of the residual DMS at peak locations and the increase of l/a, the changed amplitudes at peak locations are significant: at least

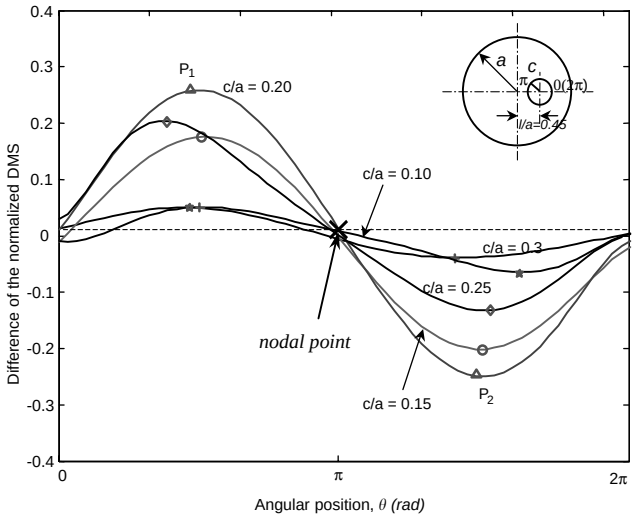

Fig. 7. Contour of DMS around the hole with c/a varying from 0.1 to 0.3.

a 15% change can be observed at p_1 and p_2 according to this figure. Moreover, for different modes, there exists a different l/a, where the amplitude of the peak will achieve its maximum for l/a varying from 0 to 1.

3.2.2. Effect of the hole size

Fig. 7 plots the contour of the residual DMS at the circumference of the hole ($l/a = 0.45$) for mode (2,0) with different hole size c/a. When c/a varies from 0.1 to 0.3, the amplitude of peaks first increases and then decreases, and two peaks around the hole can be found. With respect to Fig. 6(b), it is clear that the influence of hole size is the same as the influence of eccentricity on vibration mode around the hole. Similar results can be achieved for other modes, but they are omitted due to the limitation of length of paper.

In Fig. 7, it can be seen that a jump phenomenon exists around the hole even for a structure with a small hole; for the annular-like plate, a large hole may not necessarily result in a significant change in the residual DMS, and the locations of the peaks are variable for different c/a. These results differ from those obtained for the annular plate, for which the residual DMS is proportional to hole size, and the locations of the peaks are fixed for different c/a (Ref. [8]).

To conclude, the unobvious change in the DMS *around the hole* from global analysis can be detected clearly from local analysis. It can also give guidance on the selections of hole size and eccentricity during experimental tests.

4. Experimental modal analysis

Experiments were performed to validate simulations using the mode (1,0) of a clamped circular plate ($c/a = 0$) and a clamped–free annular-like plate ($c/a = 0.175$ and $l/a = 0.175$). The effective diameter of these two steel plates is 160 mm, with a thickness of 0.7 mm, and the diameter of the

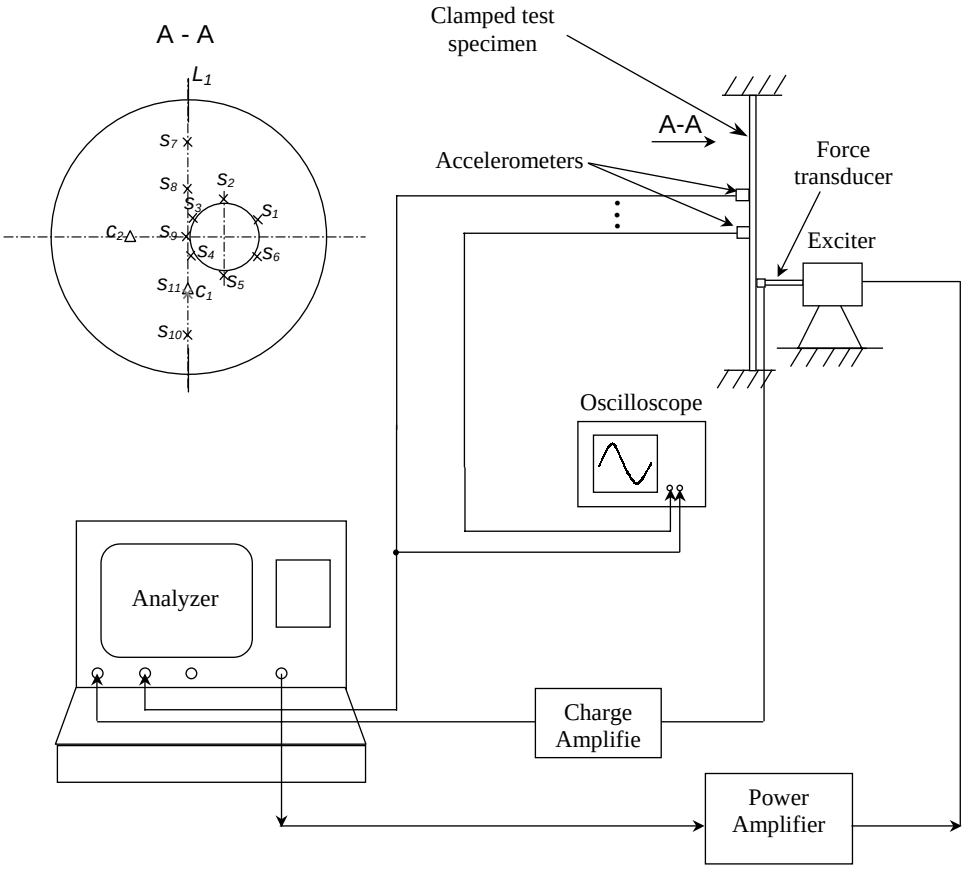

Fig. 8. Schematic diagram of the experimental set-up c_1, c_2—excitation points; $s_1, ..., s_{11}$—measurement locations.

eccentric hole is 28 mm, with an eccentricity of 14 mm for annular-like cases. The material has a Young's modulus of $E = 210\,\text{GPa}$, a density of $\rho = 7800\,\text{kg/m}^3$ and a Poisson ratio of $v = 0.3$.

4.1. Experimental set-up

Fig. 8 shows the schematic diagram of the experimental set-up used for modal testing. An excitation signal was generated by a B&K 3557 signal analyzer, then amplified by a B&K 2706 power amplifier, and exerted on the tested structure through the B&K 4810 exciter. The applied force was measured by a B&K 8203 transducer fixed between the flexible string and the plate. The vibration amplitude at the measuring locations was sensed by a B&K 4397 accelerometer, and monitored by a Tektronix TDS 220 oscilloscope. During the modal test, single-point instead of multi-point measurement was adopted to reduce the influence of the additional mass.

As mentioned above, the configuration of an ideal clamped boundary is essential to obtain good data. To realize the "clamped boundary", two flanges of radius 110 mm were aligned and located at each side of the plate (Fig. 9). Eight uniformly distributed holes of radius 4 mm were drilled at the flanges for the bolts, and two dowel pins were fitted to

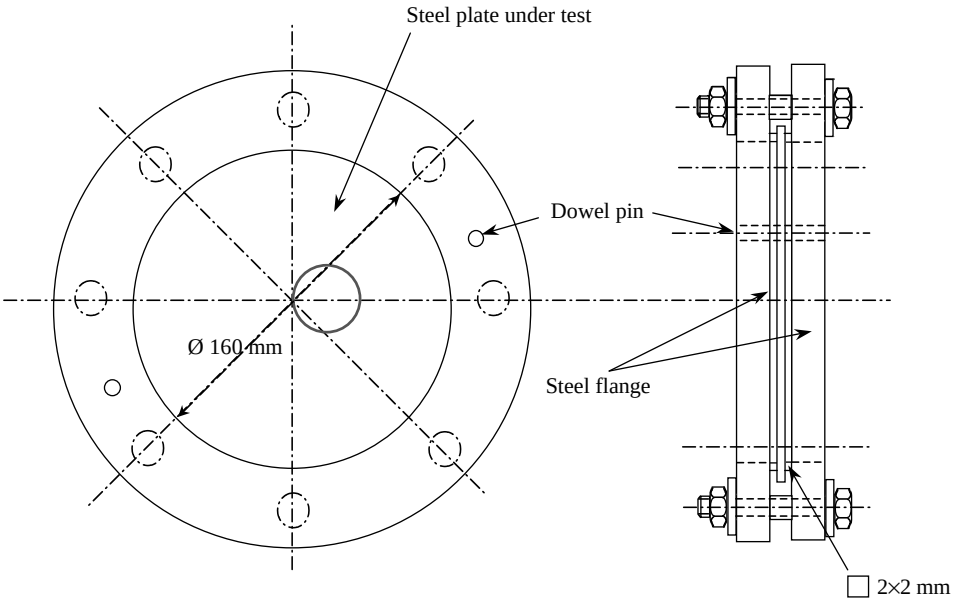

Fig. 9. Steel flange fabricated for the clamping of the steel plate under test.

ensure accurate positioning. In addition, the clamped edges, 2 mm thick and 2 mm wide, were machined along the inside diameter of the flange couples to make a rigid clamping effect.

According to the relationship between natural frequency f and eccentricity l/a, (mode (1,0) of Fig. 2(a)), for structures with a small l/a, the doublet frequency cannot be completely separated. Thus, when a certain frequency is used to generate an excitation signal, mode shapes corresponding to both frequencies may be stimulated simultaneously. Hence, the position of the excitation point during testing must be judiciously selected, with some useful methods suggested in the literature. For example, Jeong et al. thought that a good signal would be acquired when the excitation point was designated close to the supporting edge [15]. However, it is more efficient to assign the excitation point at the location of the anti-node point, to ensure that enough input energy is provided to the structure.

An issue worthy of mention is that the locations of anti-nodes for the "recessive" and "dominant" modes are different. In general, for global analysis, the excitation point will be set at a location where the "dominant" mode can be evoked, while for local analysis, it will be set at the location where the "recessive" mode can be stimulated. It should be pointed out, however, that for the annular-like plate with a small eccentricity, changes in mode shapes related to low-order frequency are unobvious, no matter whether the frequency is the "recessive" or "dominant" one (Fig. 3(b)). Therefore, when the low-frequency modes of annular-like plates with small eccentricity are utilized, the excitation point should be located at the anti-node of "recessive" modes, to ensure that the desired information can be obtained. In this test, the excitation location was set at point c_1 rather than c_2, marked in Fig. 8 for mode (1,0) for this purpose.

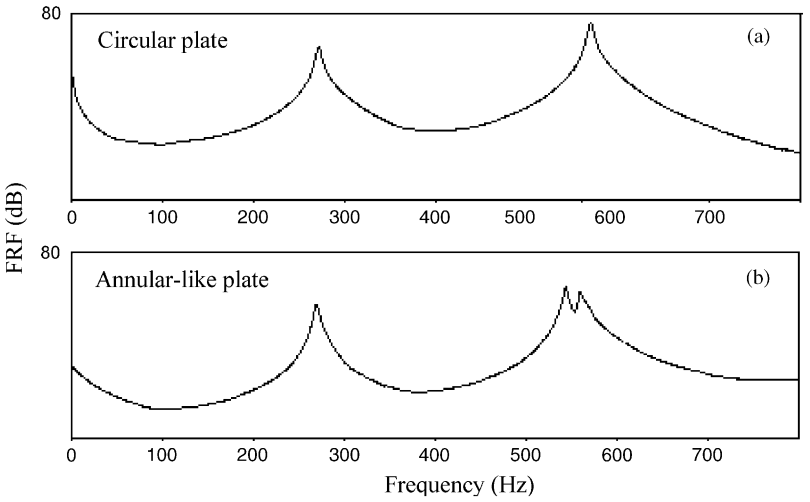

Fig. 10. Curves of frequency response function at point s_4.

Table 1
Natural frequencies of the circular and annular-like plates

Status	Mode					
	(0,0)		(1,0)			
	Experiment	Simulation	Experiment		Simulation	
Circular plate	269	273	574	574	567	567
Annular-like plate	267	274	552	568	555	561

4.2. Results and discussions

Figs. 10(a) and (b) show the curves of the frequency response function at point s_4 for the circular and annular-like plates, respectively. The *first several* natural frequencies are measured and listed in Table 1, and compared with those obtained from the numerical simulation. It can be seen that the natural frequencies obtained from the experiment are in reasonably good agreement with those obtained from the simulation, and for mode (1,0), the repeated frequency splits into two different values, with less than 3% difference.

In order to investigate the influence of a hole on the DMS, the vibration amplitudes at locations $(s_1, \ldots, s_{11})$ were measured using the input of the sinusoidal signal with $f = 574$ Hz for the circular case, and with $f = 568$ Hz for the annular-like case. In general, for mode (1,0), the amplitude should achieve its absolute maximum at locations s_{11} and s_8 theoretically. In fact, a small difference exists between these two points because of measurement errors. In this test, the maximal amplitude appeared at location s_{11}, which was taken for normalization during data processing.

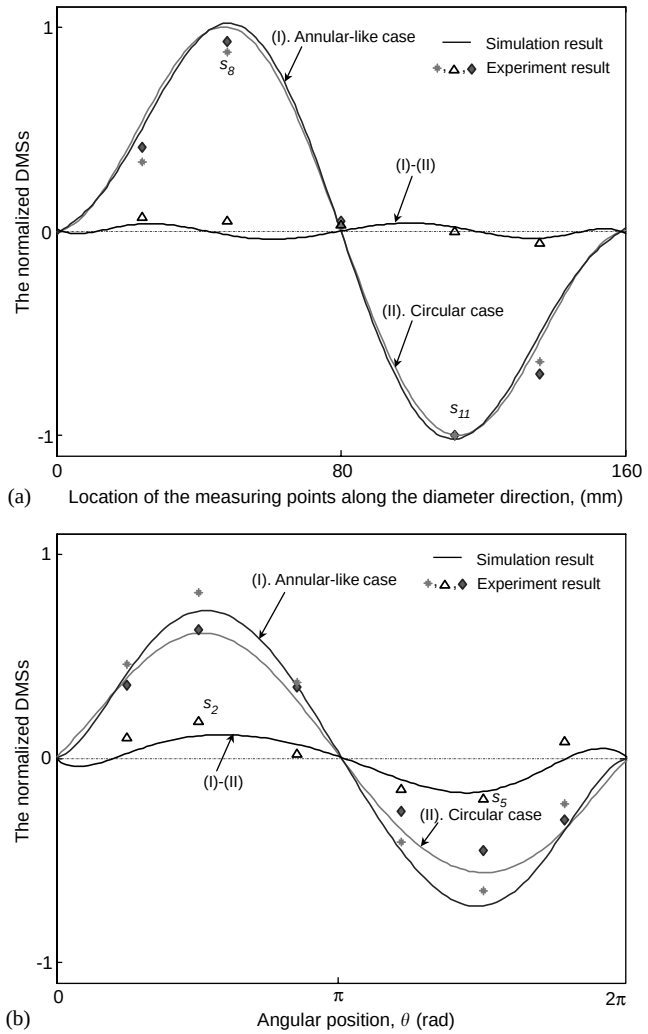

Fig. 11. The normalized DMS and the residual DMS of the tested plates for mode (1,0).

Taking the phase change into consideration, the normalized DMSs at the measurement points for mode (1,0) are plotted in Fig. 11. The simulation results are also illustrated for reference. It can be seen that

- The tendencies of the experimental data are consistent with those of numerical simulation. When the DMS is taken for analysis (Fig. 11(a) and (b): (I), (II)), the mode shapes of the circular and annular-like plate are similar, and two peaks are observed at s_8 and s_{11} among all the measured locations ($s_1, \ldots, s_{11}$). It is clear that s_8 and s_{11} are the locations where the extreme amplitudes of mode (1,0) are found. This means that when the vibration mode corresponding to the recessive frequency is adopted for vibration analysis, no obvious variation on the DMS will be perceived from the global analysis, regardless of whether or not the structure has a hole.

- When the residual DMS is used for analysis (Fig. 11(a) and (b): (I)–(II)) the peaks at s_8 and s_{11} vanish. However, two new peaks appear at s_2 and s_5. That is to say, changes can be detected at the circumference of the hole from local analysis. Apparently, the residual DMS is a sensitive parameter in indicating the location of hole.

5. Conclusions

Due to the asymmetric effect, the doublet frequency for circular plates splits into two distinct values for annular-like plates, which makes a notable difference in DMSs. In this paper, the effects of the eccentricity, hole size and boundary conditions on DMSs are investigated systematically. From the global analysis, it can be found that with increases in eccentricity or hole size, the "dominant" mode experiences distortion, while the "recessive" one remains unchanged or changes slightly. In addition, the asymmetric boundary condition results in a remarkable change in DMS compared with that obtained from the symmetric boundary. This conclusion suggests that analyses performed with perfect symmetric condition can still roughly predict the mode shapes of the "recessive" modes of plates with slightly eccentric holes. They will, however, lead to erroneous results for "dominant" modes. From the local analysis, a change in the DMSs at the circumference of the hole will be observed even for a small eccentricity or hole, while it is unobvious apart from this area. This observation indicates that the residual DMS is an effective parameter for identifying damage occurring in plate-like structures. Experimental modal tests on a clamped–free steel annular-like plate show reasonably good agreement of the results with numerical predictions.

Acknowledgements

The authors would like to thank the Research Committee of The Hong Kong Polytechnic University for its financial support for this project (Grant: GYY-27).

References

[1] J. So, A.W. Leissa, Three-dimensional vibrations of thick circular and annular plates, Journal of Sound and Vibration 209 (1998) 15–41.
[2] C.C. Lin, C.S. Tseng, Free vibration of polar orthotropic laminated circular and annular plates, Journal of Sound and Vibration 209 (1998) 797–810.
[3] A. Selmane, A.A. Lakis, Natural frequencies of transverse vibrations of non-uniform circular and annular plates, Journal of Sound and Vibration 220 (1999) 225–249.
[4] C.F. Liu, Y.T. Lee, Finite element analysis of three-dimensional vibrations of thick circular and annular plates, Journal of Sound and Vibration 233 (2000) 63–80.
[5] K.M. Liew, J.B. Han, Z.M. Xiao, Vibration analysis of circular mindlin plates using the differential quadrature method, Journal of Sound and Vibration 205 (1997) 617–630.
[6] R.H. Gutierrez, P.A.A. Laura, D.V. Bambill, V.A. Jederlinic, D.H. Hodges, Axisymmetric vibrations of solid circular and annular membranes with continuously varying density, Journal of Sound Vibration 212 (1998) 611–622.

[7] H.J. Ding, R.Q. Xu, Free axisymmetric vibration of laminated transversely isotropic annular plates, Journal of Sound Vibration 230 (2000) 1031–1044.
[8] W.O. Wong, L.H. Yam, Y.Y. Li, L.Y. Law, K.T. Chan, Vibration analysis of annular plates using mode subtraction method, Journal of Sound and Vibration 232 (2000) 807–824.
[9] H. Vinayak, R. Singh, Eigensolutions of annular-like elastic disks with intentionally removed or added material, Journal of Sound and Vibration 192 (1996) 741–769.
[10] H.B. Khurasia, S. Rawtant, Vibration analysis of circular plates with hole, Journal of Applied Mechanics—Transactions of the ASME 45 (1978) 215–217.
[11] G. Chen, J. Zhou, Vibration and Damping in Distributed Systems, Vol. II WKB and Wave Methods, Visualization and Experimentation, CRC Press, Boca Raton, FL, 1993, pp. 258–264.
[12] J.G. Tseng, J.A. Wickert, Vibration of an eccentrically clamped annular plate, Journal of Vibration and Acoustics—Transactions of the ASME 116 (1994) 155–160.
[13] A.W. Leissa, Vibration of Plates, Published for the Acoustical Society of America through the American Institute of Physics, New York, 1993, pp. 7–35.
[14] Manual: MSC/NASTRAN for Windows: Quick Start Guide. The MacNeal-Schwendler Corporation, 1995.
[15] K.H. Jeong, B.K. Ahn, S.C. Lee, Modal analysis of perforated rectangular plates in contact with water, Structural Engineering and Mechanics 12 (2001) 189–200.